31 October 2023

M2HATS 2023
Radiosonde Data Quality Report

**Holger Vömel, William Brown**
Earth Observing Laboratory
National Center for Atmospheric Research
Boulder, CO

**Earth Observing Laboratory**
**In situ Sensing Facility**

**NATIONAL CENTER FOR ATMOSPHERIC RESEARCH**
**P. O. Box 3000**
**BOULDER, COLORADO 80307-3000**

The radiosonde data for this project were quality controlled and are maintained by the Earth Observing Laboratory at the National Center for Atmospheric Research (NCAR). The National Center for Atmospheric Research is managed by the University Corporation for Atmospheric Research and sponsored by the National Science Foundation.

If information or plots from this document are used for publication or presentation purposes, please provide appropriate acknowledgement to NCAR/EOL and NSF and refer to the citation listed below. Please feel free to contact the authors for further information.

**Contacts:**

Holger Vömel (voemel@ucar.edu)
Bill Brown (wbrown@ucar.edu)

**Radiosonde operators:**

NCAR: Bill Brown, Rick Brownrigg, Reva Golden, Terry Hock, Alison McComiskey, Bruce Morley, Sam Raizman, Chris Roden, Isabel Suhr, Josh Storm, Antonio Vigil, Jacquie Witte
NorthWest Research Associates: Jielun Sun
Clemson University: Caleb Davis, Tillman Dillon, Evan Ewing, Gavin Hunt, Chenning Tong
California State University at Chico: Shane Mayor

**Mailing Address:**

NCAR/Earth Observing Laboratory
P.O. Box 3000
3090 Center Green Dr.
Boulder, CO 80301, USA

**Websites:**

M2HATS home page:
https://www.eol.ucar.edu/field_projects/m2hats
Integrated sounding system home page:
https://www.eol.ucar.edu/content/iss-operations-m2hats

**To refer to this data set or report, please include the following citation:**

NCAR/EOL In-situ Sensing Facility, Clemson University, California State University at Chico. 2023. M2HATS: ISS Radiosonde Data. Version 1.0. UCAR/NCAR - Earth Observing Laboratory. https://doi.org/10.26023/WKM7-HNCF-FX0B. Accessed 15 Nov 2023.

**Document Version Control**

| Version | Date | Author | Change Description |
|---|---|---|---|
| 1.0 | 31 Oct. 2023 | H. Vömel | Initial Data Release |
| | | | |

# 1 Table of Contents

## 2 Dataset Overview

The objective of the Multi-point Monin-Obukhov similarity horizontal array turbulence study (M2HATS) is to acquire data in the atmospheric boundary layer to test the multi-point Monin-Obukhov similarity (MMO) prediction of the surface layer similarity properties and to obtain the similarity functions. Since MMO and the original Monin-Obukhov Similarity Theory (MOST) are based on the surface layer parameters, comparisons of the MMO prediction with field measurements require predictions beyond these processes, such as the effects of the capping inversion height, the Coriolis force, and moderate baroclinicity.

The science team conducted field measurements near Tonopah, NV, between 23 July and 25 September 2023 to systematically test the predictions using field data and establish/revise the expansion coefficients and the functional forms of the MMO similarity functions.

During the campaign and the setup period, staff from NCAR/EOL, Clemson University, and the California State University at Chico successfully launched 122 radiosondes. Soundings were launched typically twice daily around 17:00 UTC and 22:00 UT (10:00 and 15:00 local time).

Only one sounding failed shortly after launch due to operator error in windy conditions. Two soundings did not provide data to the balloon ceiling due to a failure of the temperature sensor. The overall success rate of the sounding operations during this campaign was 97%. For the first time, descending data were recorded and analyzed and are available in addition to traditional ascending balloon data.

Figure 1 shows the flight tracks of all soundings until the end of telemetry reception.

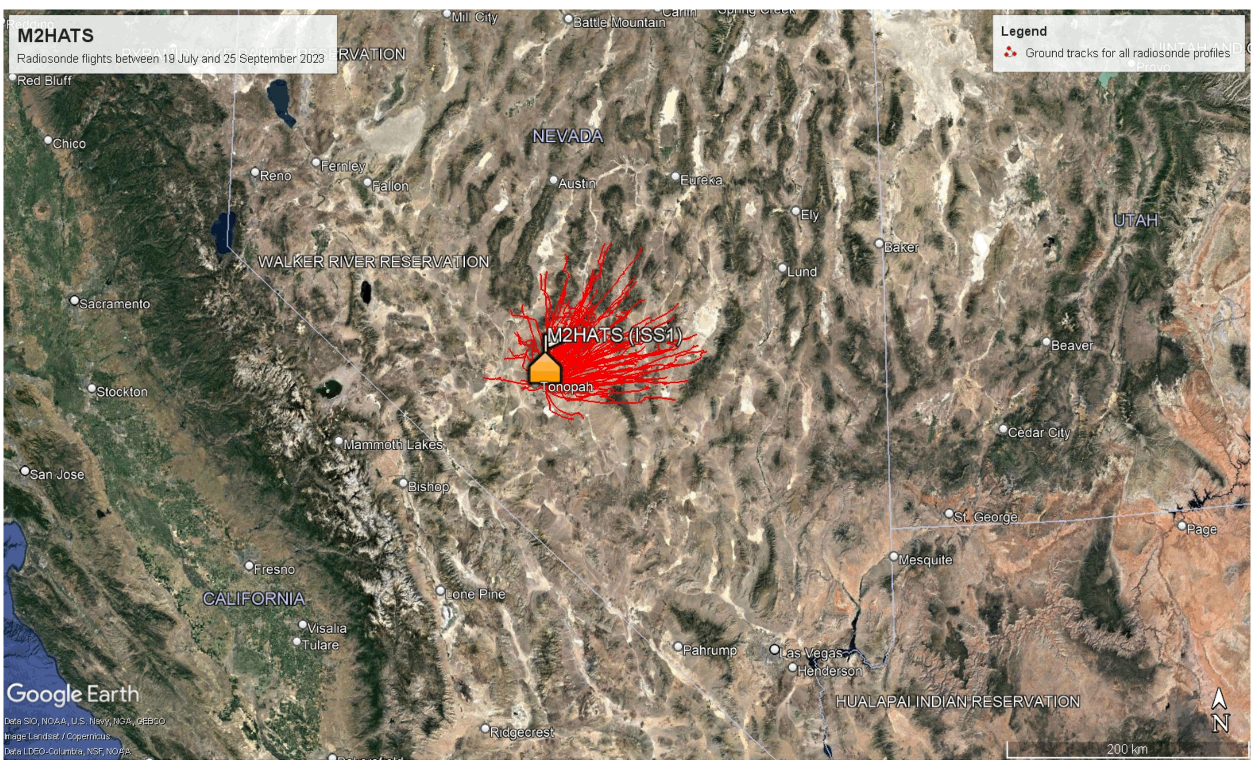


Figure 1: Location of the ISS site during M2HATS and flight tracks of all radiosonde observations. The sounding location was 12 km ESE of Tonopah, NV.

# 3 Radiosonde sounding-system

This campaign used Vaisala RS41-SGP radiosondes, which were received and processed by the Vaisala MW41 sounding system using software version 2.19.0. The radiosondes used by NCAR/EOL include a pressure sensor, which provides a better altitude and pressure determination in the boundary layer relative to pressure profiles derived from Global Navigational Satellite System (GNSS) signals received by the radiosondes. Direct pressure measurements are more suitable in the boundary layer and for unstable conditions in convective environments. The sounding system was configured to meet the needs of NCAR for high-resolution data and complete metadata description. All sondes were launched using 100 g balloons supplied by Scientific Sales.

The MWX raw data files from the sounding system were saved along with the ASCII output files, which contained the initially processed profiles.

The sounding system automatically ingests surface reference observations, which are provided by sets of reference sensors near each launch site. These observations are stored in the surface observations metadata fields of the sounding files and used in the quality control procedures of the sounding data.

The reference sensors used for the radiosonde system during M2HATS are listed in Table 1.

This campaign used a balloon inflation basket (see picture on front cover) to help balloon launch operations in windy conditions and to test the feasibility of this device for future use of hydrogen lifting gas.

Table 1: Surface reference observations provided by the ISS meteorological reference sensors during M2HATS.

| Parameter | Location | Sensor |
|---|---|---|
| Pressure | The reference pressure was installed on a mast at 2 m height near the launch site. | PTB220 |
| Temperature and humidity | The reference sensors for temperature, and humidity, were installed on a mast at 2 m height near the launch site. | Lufft WS300 |
| Wind | The reference sensor for wind speed and wind direction was installed on a mast at 10 m height near the launch site. | 2D Gill |

# 4 Quality control procedures

## 4.1 Standard quality control

The Vaisala system performs a sequence of standard quality control procedures and corrections for all radiosonde data:

- Applies a ground check correction for pressure using the pressure correction measured during the sonde preparation to compensate for small biases inherent in this type of pressure sensor.
- Performs a coarse outlier check for all measurement parameters
- Automatically detects launch based on change in pressure
- Performs a radiation correction for the temperature measurement using the radiation correction lookup table for the Vaisala RS41 radiosonde
- Corrects for response time lag of the temperature sensor
- Smooths the temperature profile
- Corrects for response time lag of the humidity sensor
- Filters out the balloon pendulum effect in the calculation of winds
- Calculates geopotential altitude based on the measured pressure profile

## 4.2 Custom quality control

In addition to the standard Vaisala procedures, all metadata are verified, and all measured parameters including reference measurements are checked for consistency and for any previously unidentified issue. The radiosonde measurements before launch are compared against the reference measurements and the causes for early termination are investigated. In the M2HATS data set, the following issues were identified and corrected:

a. In sounding 20230818_215733, launch was detected 20 s early. The additional surface data were removed in the quality controlled data.

b. The original data of the first four soundings (20230719_161344, 20230721_213732, 20230723_172736, and 20230723_215950) used an incorrect surface reference wind, which affected the wind measurements in the lowest 100 m of the soundings. The adjusted surface reference wind was used in the reprocessing and the metadata were appropriately corrected.

### 4.2.1 Ceiling altitudes

The campaign used 100 g balloons supplied by Scientific Sales and were nominally inflated with 22 $ft^3$ of He. On average balloons burst at 22.5 km. Five soundings (Table 2) terminated substantially below that. Soundings in which the sensor modules failed, did not generate descending data.

Table 2: Early sounding terminations

| Sounding | Ceiling altitude [km] | Termination reason |
|---|---|---|
| 20230804_215935 | 10.2 | PTU sensor failure |
| 20230811_220235 | 17.0 | Balloon burst |
| 20230823_165828 | 10.7 | PTU sensor failure |
| 20230916_220003 | 15.0 | Balloon burst |
| 20230920_170004 | 15.3 | Balloon burst |

### 4.2.2 Descending profiles

Four soundings (Table 3) had short sections of descending phases during the balloon ascent due to strong downdrafts. The Vaisala processing removes these downward sections. For research, they were replaced to create a continuous time series for all parameters measured by the radiosondes. The largest downward movement was observed in sounding 20230724_220030 with a temporary descent of 100 m at an altitude of 4.3 km. Downdrafts not exceeding the balloon rise rate were observed in other profiles but did not cause additional data loss in the originally processed profiles.

Table 3: Soundings showing descending sections during ascent.

| Sounding | Altitude [km] | Altitude drop [m] |
|---|---|---|
| 20230724_220030 | 4.3 | 100 |
| 20230729_215951 | 2.58 | 10 |
| 20230730_215924 | 2.7 | 5 |
| 20230903_220008 | 6.45 | 45 |

Data reception continued after balloon burst to capture the observations of the descending radiosonde. Real time ascending and descending radiosonde data were transmitted to the WMO Global Telecommunication System (GTS) in bufr format using the WMO template 3 09 057 for ascending and template 3 09 056 for descending data.

Files containing the descending portions of the soundings are included in the set of quality-controlled data. The latitude, longitude and time of the balloon burst are stored in the metadata section of the descending data files to provide the location of the beginning of the descending sounding. The time stamp in the file name was not updated, so that the connection to the ascending profile is maintained. Please use the time stamp as part of the metadata for proper timing.

The surface reference data stored in the descending sounding files repeat the surface conditions at launch.

## 4.3 File formats

The final quality-controlled data are provided in NetCDF format following the CF-1.6 metadata convention for climate and forecasting. For a detailed description of the data format, refer to Vömel et al., 2018, https://doi.org/10.5065/D65X27SR.

The file names contain the indicators ‘asc’ and ‘dsc’ for ascending or descending data.

## 5 Sounding metrics

At the M2HATS site about 12 km ESE of Tonopah, NV, 122 radiosondes were successfully launched between 19 July and 25 September 2023. With one exception, soundings were nominally launched either at 17 UT or 22 UT. Sounding 20230830_044137 was launched at night to provide a nighttime comparison with the Micro Pulse DIAL (MPD), which measured water vapor and temperature in M2HATS.

### 5.1 Height and distance

The distribution of ceiling heights is shown in Figure 2. Sounding termination heights below 19 km occurred on five soundings. Data were received as far as 131 km. The distributions of the radiosonde distances at the end of the descent data recording and at 1 km above ground is shown in Figure 3. The median distance at which a sounding was terminated was 61 km and the closest distance was 12 km. At 1 km above the ground, the median distance was 1.1 km from the launch site and all balloons were closer than 4.4 km at that altitude.

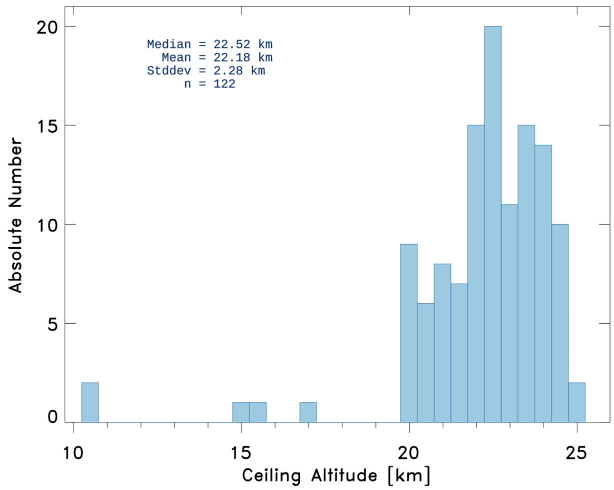


Figure 2: Distribution of ceiling heights for all radiosondes launched during M2HATS.

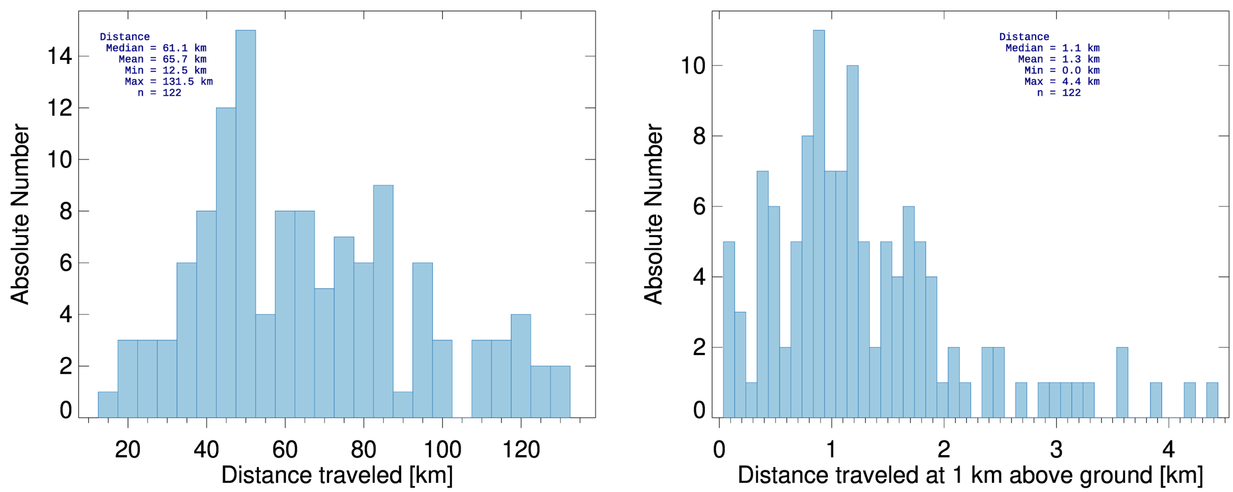


Figure 3: Distribution of balloon distance at end of data recording (left panel) and at 1 km above ground (right panel).

### 5.2 Balloon ascent rates

Balloons were typically filled with 22 $ft^3$ of helium, except for a small number of balloons that were filled with up to 25 $ft^3$ of helium. Although there is some variation, the different fill volume has no statistically detectable influence on the rise rate of the balloons.

However, the balloon performance differed strongly between those launched during the mid-morning compared to those launched in mid-afternoon (Figure 4). Balloons typically rose with between 3.5 m/s to 5.0 m/s. In the upper troposphere and stratosphere, the balloon rise rate shows no dependence on daytime. However especially below 5 km, afternoon balloons show a faster rise rate and a much larger variability compared to the morning soundings.

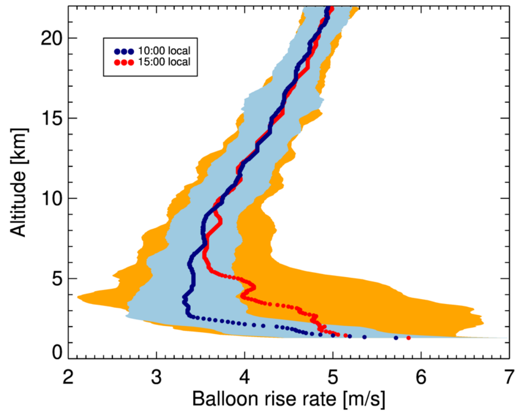


Figure 4: Average rise rates profiles for morning and afternoon soundings during M2HATS. The standard deviations of the rise rates are indicated by the shaded areas.

The sequence of all balloon rise-rates (Figure 5) frequently shows alternating fast and slow rise rates below 5 km reflecting faster rise rates in the lower troposphere in the afternoon.

Several soundings achieved rise rates of more than 10 m/s in the shallow layers between the surface and about 5 km.

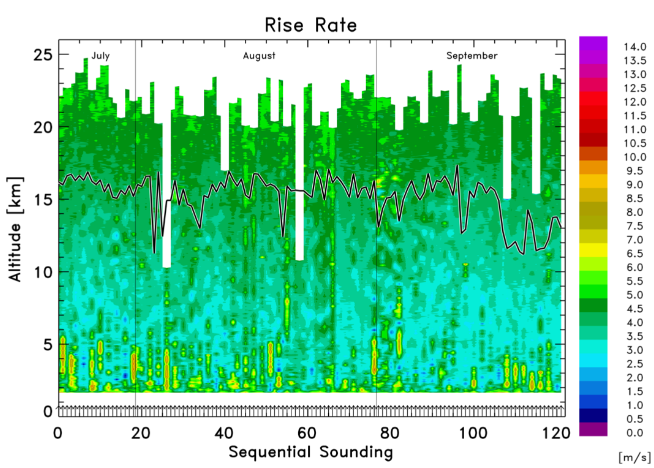


Figure 5: Sequential rise rate profiles as color contours for all radiosondes launched during M2HATS. Each launch is indicated by a small arrow at the bottom of the diagram.

### 5.3 Descent data

Data were recorded on descent and are part of the data set. In addition, descending data were sent to the GTS in real-time for models, which are capable to assimilate descending radiosonde data such as that of the European Center for Medium Range Weather Forecasting (ECMWF).

All but 7 soundings generated descending profiles down to the limit of telemetry reception. The lowest altitude from which data were received increases with increasing distance from the launch site (Figure 6). The median pressure of the end of descending profiles is 680 hPa.

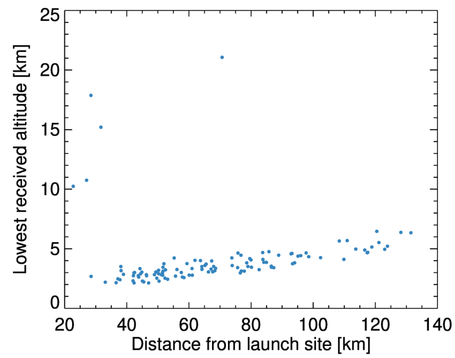


Figure 6: Lowest altitude from which data were received as function of distance from the launch site.

The quality of descending data has been investigated by Ingleby et al. (2022). Stratospheric temperature measurements on descent have a detectable warm bias relative to the ascent data. Tropospheric observations have no significant bias (Figure 7); however, due to the faster fall velocity (Figure 8), the vertical resolution is up to a factor 6 lower. Near the surface, the fall rate is approximately 13 m/s.

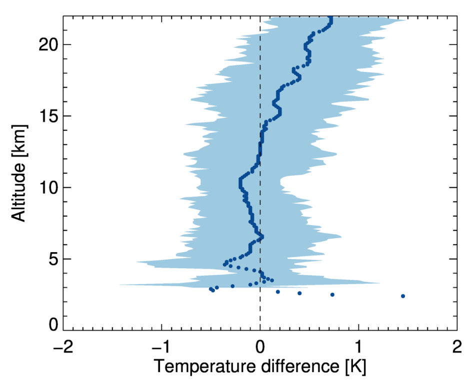


Figure 7: Difference in temperature observations between ascent and descent.

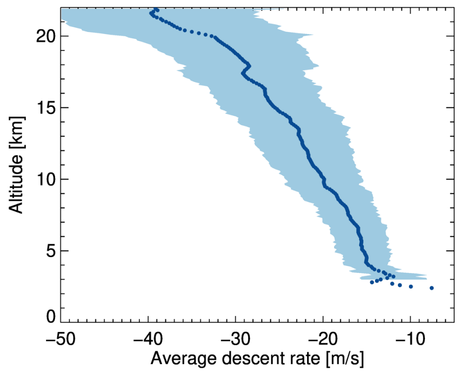


Figure 8: Average descent rate and its standard deviation for all falling radiosondes.

## 6 Atmospheric Measurements

Air temperature and relative humidity measurements from all radiosondes are shown in Figure 9. During the project, the surface temperatures at the time of the balloon launches was between 13°C and 36°C. The tropopause (shown as thin black line) ranged between about 12 and 17 km. It is also indicated by the rapid drop of relative humidity to values of less than 5%. As is customary, all relative humidity profiles are clipped at 100 % relative humidity over liquid. Profiles are shown in sequential order and span the period between 19 July and 25 September 2023. No soundings were launched on 20 and 21 August while remnants of hurricane Hilary passed over Southern Nevada, making sounding operations unsafe.

The oscillating temperatures in the boundary layer reflect the balloon launch schedule, i.e., mid-morning and mid-afternoon soundings.

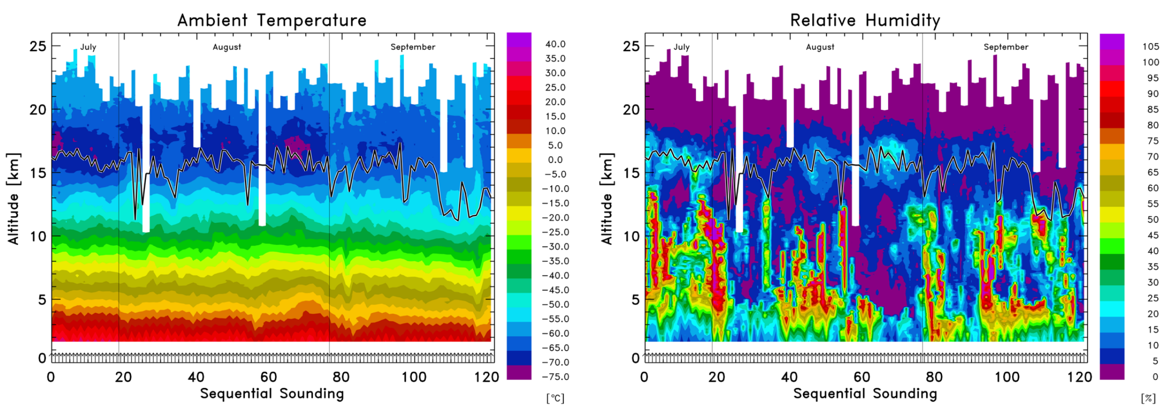


Figure 9: Sequential contours of temperature profiles (left) and relative humidity profiles (right) from all radiosondes launched during M2HATS. The tropopause is shown as thin black line typically between 12 and 17 km. Individual balloon launches are indicated by arrows at the bottom of each panel.

The zonal and meridional wind speed measurements are shown in Figure 10. The proximity of the jet stream is indicated by high wind speeds in the upper troposphere reaching up to 55 m/s. High mid tropospheric winds between soundings 52 and 56 (17 to 19 August) indicate the approaching remnants of hurricane Hilary, which passed over the site on 20 and 21 August.

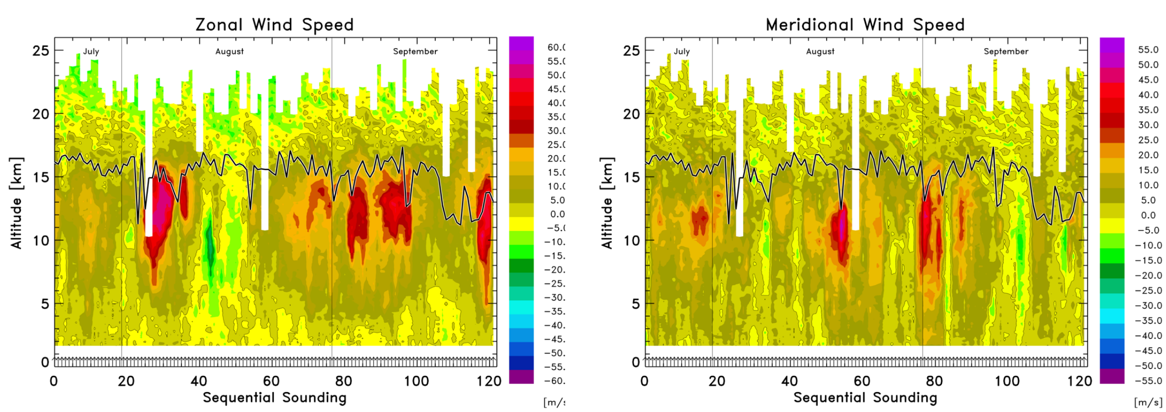


Figure 10: Time series contours of zonal and meridional wind speed profiles for all radiosondes launched during M2HATS.

The vertical wind speed is derived from the difference between the actual balloon ascent rate and the average ascent rate of all morning soundings (Figure 11). The uncertainty of this method is estimated to be about 1m/s. Strong updrafts were frequently observed in afternoon soundings, but not in morning soundings. Therefore, the average ascent rate of all morning soundings was chosen as the baseline ascent rate. w

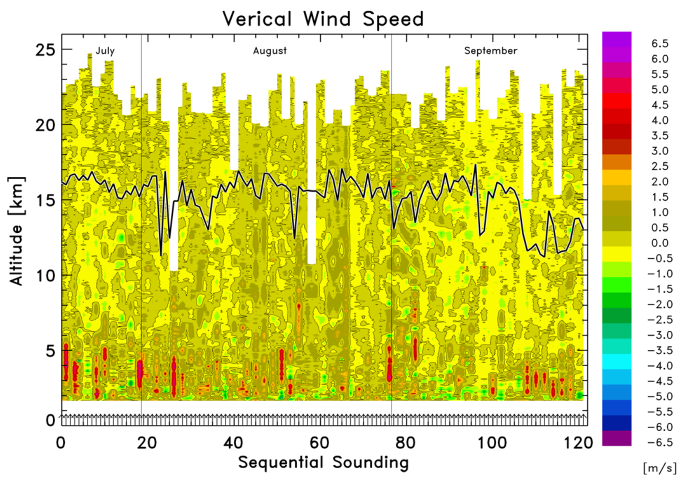


Figure 11: Sequential contours of vertical wind speed profiles.

## 7 List of all soundings

| # | Date [UTC] | Time [UTC] | Radiosonde serial number | Ceiling altitude [km] | Rise rate [m/s] | Duration [min] | Descent data |
|---|---|---|---|---|---|---|---|
| 1 | 19-Jul-23 | 16:13:44 | P0950520 | 22.1 | 4.3 | 89.5 | yes |
| 2 | 21-Jul-23 | 21:37:32 | P0950475 | 23.8 | 4.5 | 95.5 | yes |
| 3 | 23-Jul-23 | 17:27:36 | P0950464 | 22.7 | 4 | 97.8 | yes |
| 4 | 23-Jul-23 | 21:59:50 | P0950466 | 23 | 4.5 | 97 | yes |
| 5 | 24-Jul-23 | 22:00:30 | P1140646 | 25.2 | 3.9 | 101 | |
| 6 | 25-Jul-23 | 16:56:54 | P0950476 | 23.7 | 3.9 | 98.3 | yes |
| 7 | 25-Jul-23 | 21:56:34 | P0950492 | 24.7 | 3.8 | 101.1 | yes |
| 8 | 26-Jul-23 | 17:04:34 | P0950463 | 25.1 | 3.9 | 100.9 | yes |
| 9 | 26-Jul-23 | 22:15:59 | P0950465 | 22.5 | 4.3 | 97 | yes |
| 10 | 27-Jul-23 | 16:56:51 | P1140639 | 23.4 | 4.1 | 98.7 | yes |
| 11 | 27-Jul-23 | 22:03:33 | P0950368 | 24.4 | 4.3 | 98.6 | yes |
| 12 | 28-Jul-23 | 16:54:04 | P0950474 | 24.2 | 4 | 98.1 | yes |
| 13 | 28-Jul-23 | 21:53:14 | P1220021 | 24.5 | 4.2 | 97.9 | yes |
| 14 | 29-Jul-23 | 17:06:53 | P1140644 | 22 | 3.9 | 98.7 | yes |
| 15 | 29-Jul-23 | 21:59:51 | P1220053 | 21.6 | 3.9 | 97.9 | |
| 16 | 30-Jul-23 | 16:58:11 | P1220020 | 20.6 | 4 | 94.8 | yes |
| 17 | 30-Jul-23 | 21:59:24 | P1220051 | 23.7 | 3.8 | 98.2 | |
| 18 | 31-Jul-23 | 17:00:19 | P1140642 | 22.5 | 4 | 98.6 | yes |
| 19 | 31-Jul-23 | 22:08:31 | P0950486 | 21.8 | 4.4 | 92.1 | yes |
| 20 | 1-Aug-23 | 16:54:46 | P1140641 | 22 | 4.4 | 90.4 | yes |
| 21 | 1-Aug-23 | 21:55:51 | P1220054 | 22.1 | 4.1 | 95.3 | yes |
| 22 | 2-Aug-23 | 16:56:18 | P0950521 | 20.9 | 4.1 | 98.7 | yes |
| 23 | 2-Aug-23 | 21:58:01 | P0950360 | 23.1 | 4.5 | 92.6 | yes |
| 24 | 3-Aug-23 | 16:58:45 | P0950522 | 23.1 | 4 | 98.6 | yes |
| 25 | 3-Aug-23 | 21:59:25 | P1220052 | 20.2 | 4.1 | 91.7 | yes |
| 26 | 4-Aug-23 | 16:58:35 | P1140645 | 22.4 | 3.8 | 98.4 | yes |
| 27 | 4-Aug-23 | 21:59:35 | P1220022 | 10.2 | 5.6 | 25.6 | |
| 28 | 5-Aug-23 | 16:57:46 | P1220050 | 21.1 | 4 | 90.2 | yes |
| 29 | 5-Aug-23 | 21:59:25 | P1220023 | 22.7 | 4.5 | 93.5 | yes |
| 30 | 6-Aug-23 | 16:59:42 | T3340238 | 22.8 | 4.1 | 98.7 | yes |
| 31 | 6-Aug-23 | 21:59:21 | T3340240 | 22.1 | 4.3 | 93 | yes |
| 32 | 7-Aug-23 | 16:57:57 | T3340227 | 20.8 | 4.2 | 92.1 | yes |
| 33 | 7-Aug-23 | 21:57:43 | T3340224 | 20.8 | 4.4 | 88.6 | yes |
| 34 | 8-Aug-23 | 16:57:16 | T3340212 | 23.3 | 4.2 | 98.7 | yes |
| 35 | 8-Aug-23 | 21:55:06 | T3340200 | 20.7 | 4.2 | 75.4 | yes |
| 36 | 9-Aug-23 | 17:03:55 | T3340202 | 22.7 | 3.8 | 98.7 | yes |
| 37 | 9-Aug-23 | 22:01:10 | T3340215 | 22.5 | 4.1 | 98.7 | yes |
| 38 | 10-Aug-23 | 17:01:24 | T3340234 | 23.4 | 4.1 | 98.6 | yes |
| 39 | 10-Aug-23 | 21:56:37 | T3340211 | 24.2 | 3.7 | 101.9 | yes |
| 40 | 11-Aug-23 | 17:06:58 | T3340225 | 20.7 | 4 | 94.4 | yes |
| 41 | 11-Aug-23 | 22:02:35 | T3340229 | 17 | 3.9 | 79.9 | yes |
| 42 | 12-Aug-23 | 17:04:45 | U2630042 | 22.2 | 4.1 | 98.3 | yes |
| 43 | 12-Aug-23 | 21:57:29 | U2511065 | 21.6 | 4.6 | 98.6 | yes |
| 44 | 13-Aug-23 | 22:11:53 | U2620271 | 22.3 | 4.2 | 93.4 | yes |

| # | Date [UTC] | Time [UTC] | Radiosonde serial number | Ceiling altitude [km] | Rise rate [m/s] | Duration [min] | Descent data |
|---|---|---|---|---|---|---|---|
| 45 | 14-Aug-23 | 16:58:49 | U2450672 | 21.9 | 4 | 98.6 | yes |
| 46 | 14-Aug-23 | 22:01:42 | U2270228 | 20.1 | 4.8 | 80.5 | yes |
| 47 | 15-Aug-23 | 16:49:34 | U2450670 | 22.3 | 4.2 | 96.2 | yes |
| 48 | 15-Aug-23 | 22:00:29 | U2450667 | 19.9 | 4.8 | 80.9 | yes |
| 49 | 16-Aug-23 | 16:59:29 | U2510858 | 24.1 | 3.9 | 98.1 | yes |
| 50 | 16-Aug-23 | 21:57:33 | U2450671 | 22.2 | 4.5 | 91.6 | yes |
| 51 | 17-Aug-23 | 16:59:50 | U2630039 | 23.5 | 4 | 98.7 | yes |
| 52 | 17-Aug-23 | 21:58:57 | U2270260 | 23.3 | 4.3 | 98.7 | yes |
| 53 | 18-Aug-23 | 16:59:31 | U2630067 | 20.4 | 3.9 | 94.9 | yes |
| 54 | 18-Aug-23 | 21:57:33 | U2450661 | 23.4 | 4.2 | 98.2 | yes |
| 55 | 19-Aug-23 | 16:58:30 | U2630037 | 23.2 | 4 | 97.4 | yes |
| 56 | 19-Aug-23 | 21:55:28 | U2630041 | 20 | 4.8 | 73.6 | yes |
| 57 | 22-Aug-23 | 17:06:39 | U2421118 | 22.3 | 4.1 | 97 | yes |
| 58 | 22-Aug-23 | 22:00:21 | U2430856 | 21.5 | 4.5 | 83.9 | yes |
| 59 | 23-Aug-23 | 16:58:28 | U2450666 | 10.7 | 3.9 | 38.6 | |
| 60 | 23-Aug-23 | 21:59:13 | U2270148 | 22.7 | 4.2 | 95.6 | yes |
| 61 | 24-Aug-23 | 17:09:43 | U2630071 | 23 | 4 | 98.7 | yes |
| 62 | 24-Aug-23 | 22:01:47 | U2510811 | 23.9 | 3.8 | 98.6 | yes |
| 63 | 25-Aug-23 | 16:57:10 | U2270165 | 20.1 | 4.3 | 87.3 | yes |
| 64 | 25-Aug-23 | 22:05:29 | U2450821 | 21.2 | 4.1 | 95.3 | yes |
| 65 | 26-Aug-23 | 16:58:55 | U2450824 | 21 | 4.6 | 80.2 | yes |
| 66 | 26-Aug-23 | 22:03:58 | U2450829 | 24.4 | 4.3 | 98.6 | yes |
| 67 | 27-Aug-23 | 16:57:22 | U2450832 | 19.9 | 5.1 | 70.6 | yes |
| 68 | 27-Aug-23 | 22:00:08 | U2450830 | 21.2 | 3.7 | 98.6 | yes |
| 69 | 28-Aug-23 | 17:00:13 | U2450846 | 23 | 3.9 | 98 | yes |
| 70 | 28-Aug-23 | 22:00:08 | U2510398 | 23.9 | 4.1 | 98.6 | yes |
| 71 | 29-Aug-23 | 17:00:09 | U2510396 | 23.2 | 4.1 | 98.6 | yes |
| 72 | 29-Aug-23 | 22:33:38 | U2510404 | 22.4 | 4.2 | 98.7 | yes |
| 73 | 30-Aug-23 | 4:41:37 | U2510406 | 21.9 | 3.9 | 97.8 | yes |
| 74 | 30-Aug-23 | 17:00:17 | U2510414 | 22.5 | 4.2 | 96.2 | yes |
| 75 | 30-Aug-23 | 22:03:32 | U2510400 | 23.9 | 4.1 | 98.5 | yes |
| 76 | 31-Aug-23 | 17:07:19 | U2510394 | 23.5 | 4.1 | 98.7 | yes |
| 77 | 31-Aug-23 | 22:01:37 | U2510392 | 24.3 | 4.5 | 93.4 | yes |
| 78 | 1-Sep-23 | 17:07:56 | U2510403 | 22 | 4.2 | 90.8 | yes |
| 79 | 1-Sep-23 | 22:00:08 | U2510397 | 22.5 | 4.3 | 91.3 | yes |
| 80 | 2-Sep-23 | 17:00:09 | U2510391 | 22 | 4.4 | 87 | yes |
| 81 | 2-Sep-23 | 22:10:23 | U2510728 | 22.9 | 4 | 98.6 | yes |
| 82 | 3-Sep-23 | 17:06:24 | U2510408 | 21.5 | 4.1 | 95.8 | yes |
| 83 | 3-Sep-23 | 22:00:08 | U2510407 | 19.7 | 4.3 | 85.7 | |
| 84 | 4-Sep-23 | 17:01:32 | U2450826 | 21.4 | 3.9 | 98.6 | yes |
| 85 | 4-Sep-23 | 22:02:01 | U2510723 | 24.2 | 3.9 | 98.1 | yes |
| 86 | 5-Sep-23 | 17:14:10 | U2510393 | 22 | 4 | 98.7 | yes |
| 87 | 5-Sep-23 | 22:00:05 | U2510395 | 22.7 | 4.1 | 97.3 | yes |
| 88 | 6-Sep-23 | 17:01:30 | U2510386 | 21.7 | 3.9 | 98.7 | yes |
| 89 | 6-Sep-23 | 22:01:17 | U2330119 | 20.2 | 3.9 | 89.8 | yes |
| 90 | 7-Sep-23 | 17:00:07 | U2450831 | 23.8 | 3.9 | 98.1 | yes |

| # | Date [UTC] | Time [UTC] | Radiosonde serial number | Ceiling altitude [km] | Rise rate [m/s] | Duration [min] | Descent data |
|---|---|---|---|---|---|---|---|
| 91 | 7-Sep-23 | 22:00:06 | U2510387 | 24.1 | 3.9 | 98.2 | yes |
| 92 | 8-Sep-23 | 17:00:02 | U2510399 | 22.1 | 3.9 | 98.7 | yes |
| 93 | 8-Sep-23 | 22:00:04 | U2450847 | 24.5 | 4.1 | 98.1 | yes |
| 94 | 9-Sep-23 | 17:00:02 | U2450818 | 22.4 | 4.1 | 96.4 | yes |
| 95 | 9-Sep-23 | 21:58:56 | U2450823 | 24.4 | 3.7 | 102.9 | yes |
| 96 | 10-Sep-23 | 16:58:31 | U2450828 | 20.1 | 4 | 87.4 | yes |
| 97 | 10-Sep-23 | 22:03:12 | U2510401 | 24.3 | 3.9 | 98.1 | yes |
| 98 | 11-Sep-23 | 17:00:02 | U2510402 | 24.5 | 4 | 98.1 | yes |
| 99 | 11-Sep-23 | 22:00:04 | U2450817 | 21 | 3.8 | 84.8 | |
| 100 | 12-Sep-23 | 17:00:42 | U2450827 | 22.7 | 3.7 | 98.1 | yes |
| 101 | 12-Sep-23 | 22:00:06 | U2450825 | 20.3 | 3.9 | 95.9 | yes |
| 102 | 13-Sep-23 | 17:00:03 | U2450834 | 24.1 | 3.8 | 98.4 | yes |
| 103 | 13-Sep-23 | 22:04:17 | U2450833 | 21.8 | 3.8 | 98.7 | yes |
| 104 | 14-Sep-23 | 17:05:41 | V1250005 | 22.3 | 3.8 | 98.6 | yes |
| 105 | 14-Sep-23 | 22:00:05 | V1241409 | 23.6 | 4 | 98.7 | yes |
| 106 | 15-Sep-23 | 17:00:11 | V1240108 | 23.6 | 4 | 98.7 | yes |
| 107 | 15-Sep-23 | 22:00:04 | V1241347 | 23.2 | 3.8 | 98.5 | yes |
| 108 | 16-Sep-23 | 17:00:06 | V1241426 | 20.7 | 3.7 | 98.7 | yes |
| 109 | 16-Sep-23 | 22:00:03 | V1241425 | 15 | 3.9 | 98.6 | yes |
| 110 | 17-Sep-23 | 17:00:04 | V1241423 | 23.4 | 4 | 98.6 | yes |
| 111 | 17-Sep-23 | 22:00:03 | V1241407 | 20.7 | 4.2 | 90.3 | yes |
| 112 | 18-Sep-23 | 17:00:05 | V1241424 | 24.6 | 3.9 | 98.2 | yes |
| 113 | 18-Sep-23 | 22:00:02 | V1241325 | 22.6 | 4.1 | 96.7 | yes |
| 114 | 19-Sep-23 | 17:00:02 | V1241346 | 24 | 3.9 | 98.3 | yes |
| 115 | 19-Sep-23 | 22:00:08 | V1241310 | 22 | 4.1 | 95.7 | yes |
| 116 | 20-Sep-23 | 17:00:04 | V1241428 | 15.3 | 3.6 | 83.7 | yes |
| 117 | 20-Sep-23 | 22:00:03 | V1241427 | 23.6 | 4.3 | 98.3 | yes |
| 118 | 21-Sep-23 | 17:12:15 | V1241349 | 24 | 4.1 | 98.2 | yes |
| 119 | 21-Sep-23 | 22:00:03 | V1241206 | 22.5 | 4.3 | 92.9 | yes |
| 120 | 22-Sep-23 | 17:00:15 | V1241311 | 23.8 | 4 | 98.4 | yes |
| 121 | 22-Sep-23 | 21:56:07 | V1241312 | 23.6 | 3.9 | 98.4 | yes |
| 122 | 25-Sep-23 | 16:33:44 | V1241410 | 23.3 | 4 | 98.6 | yes |

## 8 References

Ingleby, B., Motl, M., Marlton, G., Edwards, D., Sommer, M., von Rohden, C., Vömel, H., and Jauhiainen, H. (2022): On the quality of RS41 radiosonde descent data, Atmos. Meas. Tech., 15, 165–183, https://doi.org/10.5194/amt-15-165-2022

Vömel, H., G. Granger, and I. Suhr, 2018, NCAR/EOL/ISF Radiosonde NetCDF Data Files, UCAR/NCAR - Earth Observing Laboratory. https://doi.org/10.5065/D65X27SR.